 CMC, vol.43, no.2, pp.97-108, 2014

Magneto-Mechanical Finite Element Analysis of Single Crystalline Ni_2MnGa Ferromagnetic Shape Memory Alloy

Yuping Zhu[1,2], Tao Chen[1] and Kai Yu[1]

Abstract: Based on an existing micromechanical constitutive model for Ni_2MnGa ferromagnetic shape memory alloy single crystals, a three-dimensional quasi-static isothermal incremental constitutive model that is suitable for finite element analysis is derived by using Hamilton's variational principle. This equation sets up the coupling relation between the magnetic vector potential and the mechanical displacement. By using the incremental equation and ANSYS software, the mechanical behaviors of martensitic variant reorientation for Ni_2MnGa single crystals are analyzed under magneto-mechanical coupling action. And the finite element results agree well with the experimental data. The methods used in the paper can well describe the mechanical behaviors of the material in complex fields.

Keywords: Ferromagnetic shape memory alloy, Magneto-mechanical coupling, Finite element analysis, Mechanical behaviors.

1 Introduction

Shape memory alloy is a kind of important intelligent materials [Kanca and Eskil (2009)]. Ferromagnetic shape memory alloys (FSMAs), represented by Ni_2MnGa, have been intensively researched since 1996. FSMAs may generate strain under magnetic field, temperature or stress. The magnetic field-induced strain of single crystalline Ni_2MnGa has evolved from initially reported 0.2% [Ullakko and Huang (1996)] to 10% [Karaca, Karaman, Basaran and Lagoudas (2007)], which makes it possible to the use in intelligent structure.

Single crystalline Ni_2MnGa has abundant microstructures. Shape memory effect and super-elastic properties of FSMAs have to do with microstructure of the material.In order to deeply investigate its mechanical behaviors, many people have developed lots of constitutive models [Kieer and Lagoudas (2005); Pei and Fang (2007); Wang, Li and Hu (2012); Zhu and Yu (2013); Zhu, Shi and Wang (2013)].

[1] Institute of Mechanics & Engineering, Jiangsu University, Zhenjiang 212013, China.
[2] Corresponding author. Tel: +86 511-88780197; E-mail: zhuyuping@126.com

Due to its anisotropic mechanical behaviors and nonlinear constitutive relation, it is difficult to obtain the analytical solution of its constitutive equation. Moreover, only simple magneto-mechanical coupling experiments can be achieved, which has limited further researches of this material.

Finite element analysis (FEA) is widely used in the analysis of the traditional shape memory alloy [Casciati, et al. (2011); Chen, et al. (2012)], and has been used to analyze the mechanical behaviors of single crystalline FSMAs. Kiang and Tong [Kiang and Tong (2007); Kiang and Tong (2009)] derived a two-dimensional constitutive model for FEA, and verified the relation between the magnetic field and the strain under constant stresses. However, this constitutive model fails to reflect the effect of the shape of martensitic variants and the material properties on the macroscopic material properties. Wang and Steinmann[Wang and Steinmann (2013)] proposed a new constitutive model for FEA, gave an iterative method to solve the constitutive equation, and described the magnetization distribution, volume fractions of variants and stress-strain curves. Lagoudas et al. [Lagoudas, Kiefer and Haldar (2008)] employed the COMSOL software to analyze the effect of non-uniformly distributed magnetic force on stress distribution. As we all know, single crystalline Ni_2MnGa has rich microstructures, which may affect mechanical behavires of FSMA. However, most above FSMAs constitutive models fail to reflect the characteristics very well.

Based on micromechanics and thermodynamics, Zhu and Dui [Zhu and Dui (2008)] established a three-dimensional constitutive model for single crystalline FSMAs, the model reflects the effect of the microscopic evolution on the macroscopic properties.

Based on the micromechanical model in Reference [Zhu and Dui (2008)] and Hamilton's variational principle, we will derive a discretized incremental model suitable for FEA, namely, a three-dimensional quasi-static isothermal incremental finite element formula for martensitic variant reorientation. The formula establishes the coupling relation between the magnetic vector potential and the mechanical displacement. Employing the FEA software ANSYS, the programming language Fortran, and the above incremental equations, and writing a finite element subroutine for the custom material, we analyze the mechanical behaviors during martensitic variant reorientation of Ni_2MnGa single crystals under magneto-mechanical coupling action.

2 Hamilton's variational principle

According to Hamilton's variational principle, the dynamic equation in variational form is [Chari and Salon (2005); Honig (1999); O'Handley (2000)]

$$\delta \int_t (L+W)\mathrm{d}t = \int_t (\delta K - \delta P + \delta W)\mathrm{d}t = 0 \tag{1}$$

where L is the Lagrangian, W is the external work, P is the internal energy, K is the kinetic energy, and t represents the time domain.

For a general magneto-mechanically coupled material, the internal energy is [8,9]

$$\delta \int_t \int_v P\mathrm{d}v\mathrm{d}t = \int_t \int_v \{\sigma\}^{\mathrm{T}} \{\delta\varepsilon\}\mathrm{d}v\mathrm{d}t + \int_t \int_v \{H\}^{\mathrm{T}} \{\delta B\}\mathrm{d}v\mathrm{d}t \tag{2}$$

where $\{\sigma\}$ is the stress, $\{\delta\varepsilon\}$ is the strain variation, $\{H\}$ is the magnetic field intensity, $\{\delta B\}$ is the magnetic induction variation, and v denotes volume. And the external work is

$$\begin{aligned} &\delta \int_t \int_v W\mathrm{d}v\mathrm{d}t = \int_t \int_v \{\delta u\}^{\mathrm{T}} \{F_v\}\,\mathrm{d}v\mathrm{d}t + \int_t \int_v \{\delta A\}^{\mathrm{T}} \{J\}\,\mathrm{d}v\mathrm{d}t \\ &+ \int_t \int_s \{\delta u\}^{\mathrm{T}} \{F_s\}\,\mathrm{d}s\mathrm{d}t + \int_t \{\delta u\}^{\mathrm{T}} \{F_p\}\,\mathrm{d}t \end{aligned} \tag{3}$$

where $\{\delta u\}$ is the displacement variation, $\{F_p\}$ is the point force, $\{F_s\}$ is the surface force, $\{F_v\}$ is the body force, $\{\delta A\}$ is the magnetic vector potential variation, $\{J\}$ is the current density, and s denotes area.

Neglect the kinetic energy and gravity. Substituting Eqs. (2) and (3) into (1) yields

$$\begin{aligned} &-\delta \int_t \int_v P\mathrm{d}v\mathrm{d}t + \delta \int_t \int_v W\mathrm{d}v\mathrm{d}t = \int_t \int_v \{\delta A\}^{\mathrm{T}} \{J\}\,\mathrm{d}v\mathrm{d}t + \\ &\int_t \{\delta u\}^{\mathrm{T}} \{F_p\}\,\mathrm{d}t - \int_t \int_v \{\sigma\}^{\mathrm{T}} \{\delta\varepsilon\}\,\mathrm{d}v\mathrm{d}t - \int_t \int_v \{H\}^{\mathrm{T}} \{\delta B\}\,\mathrm{d}v\mathrm{d}t = 0 \end{aligned} \tag{4}$$

The incremental expression of (4) is

$$\begin{aligned} &\int_t \{\delta u\}^{\mathrm{T}} \{\Delta F_p\}\,\mathrm{d}t + \int_t \int_v \{\delta A\}^{\mathrm{T}} \{\Delta J\}\,\mathrm{d}v\mathrm{d}t - \int_t \int_v \{\delta\varepsilon\}^{\mathrm{T}} \{\Delta\sigma\}\,\mathrm{d}v\mathrm{d}t \\ &- \int_t \int_v \{\delta B\}^{\mathrm{T}} \{\Delta H\}\,\mathrm{d}v\mathrm{d}t = 0 \end{aligned} \tag{5}$$

where

$$\{\delta u\} = \begin{pmatrix} \delta u_x & \delta u_y & \delta u_z \end{pmatrix}^{\mathrm{T}}, \quad \{\Delta F_p\} = \begin{pmatrix} \Delta F_x & \Delta F_y & \Delta F_z \end{pmatrix}^{\mathrm{T}},$$
$$\{\delta \mathrm{A}\} = \begin{pmatrix} \delta \mathrm{A}_x & \delta \mathrm{A}_y & \delta \mathrm{A}_z \end{pmatrix}^{\mathrm{T}}, \quad \{\Delta J\} = \begin{pmatrix} \Delta J_x & \Delta J_y & \Delta J_z \end{pmatrix}^{\mathrm{T}},$$
$$\{\delta \varepsilon\} = \begin{pmatrix} \delta \varepsilon_{\mathrm{x}} & \delta \varepsilon_{\mathrm{y}} & \delta \varepsilon_{\mathrm{z}} & \delta \gamma_{\mathrm{yz}} & \delta \gamma_{\mathrm{xz}} & \delta \gamma_{\mathrm{xy}} \end{pmatrix}^{\mathrm{T}},$$
$$\{\Delta \sigma\} = \begin{pmatrix} \Delta \sigma_x & \Delta \sigma_y & \Delta \sigma_z & \Delta \tau_{yz} & \Delta \tau_{xz} & \Delta \tau_{xy} \end{pmatrix}^{\mathrm{T}},$$
$$\{\delta \mathrm{B}\} = \begin{pmatrix} \delta \mathrm{B}_x & 0 & \delta \mathrm{B}_y & 0 & \delta \mathrm{B}_z & 0 \end{pmatrix}^{\mathrm{T}},$$
$$\{\Delta \mathrm{H}\} = \begin{pmatrix} \Delta \mathrm{H}_x & 0 & \Delta \mathrm{H}_y & 0 & \Delta \mathrm{H}_z & 0 \end{pmatrix}^{\mathrm{T}}$$

3 The constitutive model in incremental format

This paper is based on the constitutive model of literature [Zhu and Dui (2008)], the constitutive model is explained as follow.

According to Reference [Zhu and Dui (2008)], assume a single crystalline Ni_2MnGa is completely martensitic variant 1 initially. An external field **H** leads to martensitic variant reorientation, generating variant 2, see Fig.1.

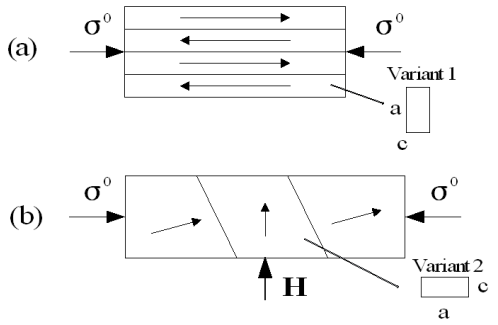

Figure 1: Schematic of a Ni_2MnGa single-crystal sample under field and stress [Kieer and Lagoudas (2005); Zhu and Dui (2008)].

For convenience, assume that these two martensitic variants share the same elastic modulus matrix $[\mathbf{L}_0]$. Then the macroscopic strain is [Zhu and Dui (2008)]

$$\{\varepsilon\} = [\mathbf{L}_0]^{-1}\{\sigma\} + \xi\{\varepsilon^r\} \tag{6}$$

where ξ is the volume fraction of variant 2, $\{\varepsilon^r\}$ is the reorientation strain. ξ is decided by thermodynamics. Assume that the entropy is constant during martensitic variant reorientation, and the Gibbs free energy only includes the mechanical

potential energy. Other free energy are neglected. When the direction of the magnetic field is perpendicular to the stress, the kinetic equation of martensitic variants reorientation is [Zhu and Dui (2008)]

$$\frac{1}{2}(1-2\xi)[\mathbf{L}_0]([\mathbf{S}]-[\mathbf{I}])\{\varepsilon^{\mathrm{r}}\}\{\varepsilon^{\mathrm{r}}\}+\{\sigma\}\cdot\{\varepsilon^{\mathrm{r}}\}+\mu_0 M^{\mathrm{sat}}\bar{H}=2\gamma_s/t+h\xi \tag{7}$$

where γ_s is the surface energy density,t is the thickness of the martensite plate, M^{sat} is the saturation magnetization decided by experiment, h is an undetermined constant, [**S**] is the Eshelby tensor, and [**I**] is the identity tensor of 4-order. In order to make calculation easier, the dissipated energy in Reference [Zhu and Dui (2008)] is simplified as linear, which used in many literatures on shape mempry alloy [Kieer and Lagoudas (2005)].

The incremental form of Eq.(6) is

$$\{\Delta\varepsilon\}=[\mathbf{L}_0]^{-1}\{\Delta\sigma\}+\{\varepsilon^r\}\Delta\xi \tag{8}$$

From Eq. (7)

$$\Delta\xi=\frac{\partial\xi}{\partial\bar{\sigma}}\Delta\bar{\sigma}+\frac{\partial\xi}{\partial\bar{H}}\Delta\bar{H} \tag{9}$$

where $\Delta\bar{\sigma}$ and $\Delta\bar{H}$ denote the incremental stress and the magnetic field intensity respectively.

$$\frac{\partial\xi}{\partial\bar{\sigma}}=\varepsilon^r/h+[\mathbf{L}_0]([\mathbf{S}]-[\mathbf{I}])\{\varepsilon^r\}\{\varepsilon^r\} \tag{10}$$

$$\frac{\partial\xi}{\partial\bar{H}}=\mu_0 M^{\mathrm{sat}}\Big/h+[\mathbf{L}_0]([\mathbf{S}]-[\mathbf{I}])\{\varepsilon^r\}\{\varepsilon^r\} \tag{11}$$

The incremental constitutive model for single crystalline Ni_2MnGa derived from Eq. (8) and Eq. (9) is

$$\{\Delta\sigma\}_{i+1}=[\mathbf{L}]_i^{-1}\{\Delta\varepsilon\}_{i+1}-[\mathbf{C}]_i\{\Delta H\}_{i+1} \tag{12}$$

where

$$[\mathbf{L}]=[\mathbf{L}_0]^{-1}+[\varepsilon^r]\frac{\partial\xi}{\partial\bar{\sigma}},\quad [\mathbf{C}]=[\mathbf{L}]^{-1}[\varepsilon^r]\frac{\partial\xi}{\partial\bar{H}},\quad \{\Delta H\}_{i+1}=[\mathbf{P}_0]\{\Delta B\}_{i+1} \tag{13}$$

where μ_0 is the permeability of free space, and $[\mathbf{P}_0]$ is given in the Appendix.

In FEA, a displacement interpolation for a K-node element is

$$\{u\}=[N]\{u_e\} \tag{14}$$

where $\{u\}$ is the displacement vector of a point, $\{u_e\}$ is the nodal displacement vector of the element, and $[N]$ is the shape function matrix (see the Appendix).A strain interpolation for a K-node element is

$$\{\varepsilon\} = [Z]_u \{u_e\} \tag{15}$$

where $\{\varepsilon\}$ is the strain vector of a point, $[Z]_u$ is the strain matrix (see the Appendix). Similarly, interpolations of $\{A\}$ and $\{B\}$ are

$$\begin{aligned} \{A\} &= [N]\{A_e\} \\ \{B\} &= [Z]_A \{A_e\} \end{aligned} \tag{16}$$

where $[Z]_A$ is in the Appendix.

Substituting Eqs. (8) $\sim$ (16) into Eq. (5), results in the FEA formula in incremental format

$$\begin{aligned} &\int \left(\begin{array}{l} \{\delta u_e\}_{i+1}^{\mathrm{T}} [K_{uu}]_i \{\Delta u_e\}_{i+1} - \{\delta u_e\}_{i+1}^{\mathrm{T}} [K_{uA}]_i \{\Delta A_e\}_{i+1} \\ + \{\delta A_e\}_{i+1}^{\mathrm{T}} [K_{Au}]_i \{\Delta u_e\}_{i+1} + \{\delta A_e\}_{i+1}^{\mathrm{T}} [K_{AA}]_i \{\Delta A_e\}_{i+1} \end{array} \right) \mathrm{d}t \\ &= \int \{\delta u_e\}_{i+1}^{\mathrm{T}} \{\Delta F_e\}_{i+1} \, \mathrm{d}t + \{\delta A_e\}_{i+1}^{\mathrm{T}} \int [N]^{\mathrm{T}} \{\Delta J\}_{i+1} \, \mathrm{d}t \end{aligned} \tag{17}$$

where

$$[K_{uu}]_i = \left\{ \begin{array}{ll} \int [Z]_u^{\mathrm{T}} [\mathbf{L}_0] [Z]_u \, \mathrm{d}v & \text{(linear)} \\ \int [Z]_u^{\mathrm{T}} [\mathbf{L}]^{-1} [Z]_u \, \mathrm{d}v & \text{(nonlinear)} \end{array} \right. \tag{18}$$

$$[K_{uA}]_i = \left\{ \begin{array}{ll} 0 & \text{(linear)} \\ \int [Z]_u^{\mathrm{T}} [\mathbf{C}] [\mathbf{P}]_0 [Z]_A \, \mathrm{d}v & \text{(nonlinear)} \end{array} \right. \tag{19}$$

$$[K_{Au}]_i = \left\{ \begin{array}{ll} 0 & \text{(linear)} \\ 0 & \text{(nonlinear)} \end{array} \right. \tag{20}$$

$$[K_{AA}]_i = \left\{ \begin{array}{ll} \int [Z]_A^{\mathrm{T}} [\mathbf{P}]_0 [Z]_A \, \mathrm{d}v & \text{(linear)} \\ \int [Z]_A^{\mathrm{T}} [\mathbf{P}]_0 [Z]_A \, \mathrm{d}v & \text{(nonlinear)} \end{array} \right. \tag{21}$$

Rearrange Eq. (17) into

$$\left(\begin{array}{cc} [K_{uu}] & [K_{uA}] \\ 0 & [K_{AA}] \end{array} \right)_i \left(\begin{array}{c} \Delta u_e \\ \Delta A_e \end{array} \right)_{i+1} = \left(\begin{array}{c} \{\Delta F_e\} \\ \{\Delta I_e\} \end{array} \right)_{i+1} \tag{22}$$

where

$$I_e = \int [N]^{\mathrm{T}} \{J\} \, dv \tag{23}$$

4 Numerical calculations

As the ANSYS core program is in the Fortran language, we write a finite element subroutine in Fortran 90 for the derived three-dimensional quasi-static isothermal finite element formula (22), then compares the simulation results to the experimental data. The single crystalline Ni_2MnGa sample adopted in this paper is 10×5 mm^2. And according to the characteristics of the structure, the SOLID62 Magneto-Structural 8-node hexahedron element is chosen.

4.1 The FEA results under constant stresses

This section adopts $Ni_{51.3}Mn_{24.0}Ga_{24.0}$, whose material constants are in Table 1 [Kieer and Lagoudas (2005); Tickle (2000)]. In the table, $H^{s(1,2)}$ ($H^{f(1,2)}$) denotes the threshold magnetic field for the start and finish reorientation from variant 1 to variant 2, $H^{s(2,1)}$ ($H^{f(2,1)}$) denotes the threshold magnetic field for the start and finish of the reverse reorientation from variant 2 to variant 1 under -1MPa, and ε^r denotes the maximum reorientation strain under different stress.

Table 1: Material constants for a $Ni_{51.3}Mn_{24.0}Ga_{24.0}$ specimen [Kieer and Lagoudas (2005); Tickle (2000)].

Quantity	Value (unit)	Quantity	Value (unit)
μ_0	1.256 μNA^{-2}	$H^{s(1,2)}$(-1 MPa)	232 kA/m
M^{sat}	622 kA/m	$H^{f(1,2)}$(-1 MPa)	1250 kA/m
ε^r (-1 MPa)	0.02148	$H^{s(2,1)}$(-1 MPa)	580 kA/m
ε^r(-3 MPa)	0.0133	$H^{f(2,1)}$(-1 MPa)	0
ε^r(-5 MPa)	0.0034		

Fig. 2 compares results of FEA with experiment data under different constant compressive stresses. The curve of -1 MPa is simulated, in order to decide material constants, whereas curves of -3 MPa and -5 MPa are predicted. Dot curves are from experiment [Tickle (2000)] while solid curves are from FEA. Fig. 2 shows that the smaller the compressive stress, the greater the reorientation strain. The FEA results match Reference [Tickle (2000)] well, and the hysteresis of macroscopic response is well reflected.

4.2 The FEA results under constant magnetic fields

This section adopts $Ni_{49.7}Mn_{29.1}Ga_{21.2}$, whose material constants are in Table 2 [Straka and Heczko (2003)], where $\sigma^{s(1,2)}$ ($\sigma^{f(1,2)}$) denotes the threshold stress

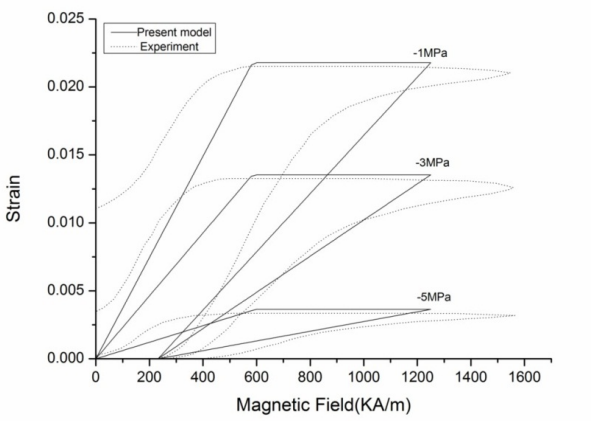

Figure 2: Comparison of finite element results and experimental data under different constant stress.

for the start and finish of reorientation from variant 1 to variant 2, $\sigma^{s(2,1)}$ ($\sigma^{f(2,1)}$) denotes the threshold stress for the start and finish of reverse reorientation from variant 2 to variant 1, and ε^r denotes the reorientation strain under 0.6 T.

Table 2: Material constants for a $Ni_{49.7}Mn_{29.1}Ga_{21.2}$ specimen [Straka and Heczko (2003)].

Quantity	Value (unit)	Quantity	Value (unit)
μ_0	1.256 μNA^{-2}	$\sigma^{f(1,2)}$(0.6 T)	5.4 MPa
M^{sat}	570 kA/m	$\sigma^{s(2,1)}$(0.6 T)	1.7 MPa
ε^r	0.0576	$\sigma^{f(2,1)}$(0.6 T)	0 MPa
$\sigma^{s(1,2)}$(0.6 T)	2.3 MPa		

Compare the FEA results with the experimental data under different constant magnetic fields, as shown in Fig. 3. The curve of 0.6 T is simulated, in order to decide material constants. Dot curves are from experiment [Straka and Heczko (2003)], while solid curves are from FEA. Fig. 3(a) gives the stress-strain curves under greater constant magnetic fields 0.6 T and 0.9 T, while Fig. 3(b) gives the stress-strain curves under smaller constant magnetic fields 0 T, 0.2 T and 0.3 T. As seen in Fig.3, the nonlinear and hysteretic strain response of FSMAs can be investigated well for stress-induced reorientation under constant magnetic field. Fig. 3 shows that the greater the magnetic field intensity the greater the threshold stress and the smaller the residual strain. From Fig.3, it is evident that the FEA results is in good

agreement with the experimental data. The results of Fig. 2 and Fig.3 show the feasibility of the present method.

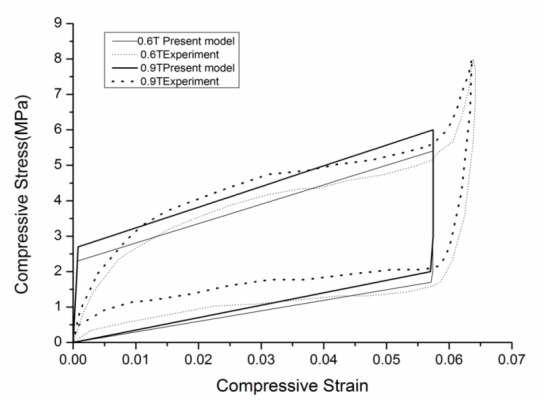

(a) For greater magnetic fields

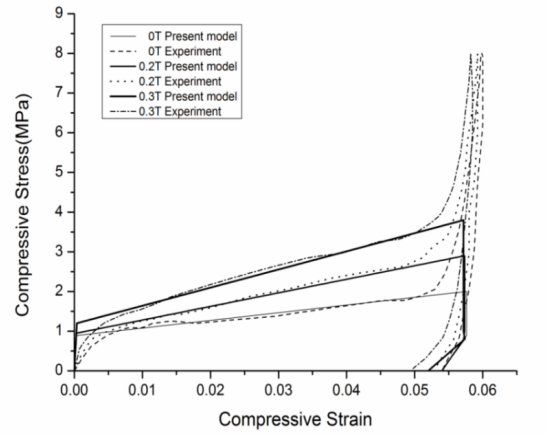

(b) For zero and smaller magnetic fields

Figure 3: Comparison of finite element results with experiment under different constant magnetic fields.

5 Conclusions

Based on an existing micromechanical constitutive model and Hamilton's variational principle, we develop a three-dimensional quasi-static isothermal incremental finite element formula of FSMAs during martensitic variant reorientation. Employing the FEA software ANSYS, the programming language Fortran, and the

derived incremental equation, we analyze the strain vs. magnetic field under different constant compressive stresses and stress-strain curves under different constant magnetic fields. And compares the FEA results with the experimental data. The FEA results agree well with the experimental data. The present method can well describe the nonlinear and hysteresis macroscopic response, which proves the feasibility of the FEA programming. Furthermore, we may use the present method to investigate the mechanical properties of FSMAs material under complex fiedls.

Acknowledgement: The authors wish to thank the National Natural Science Foundation of China (No. 11272136).

References

Casciati, F.; Casciati, S.; Faravelli, L.; Marzi, A. (2011): Fatigue damage accumulation in a Cu-based shape memory alloy: Preliminary investigation. *CMC-Computers, Materials, & Continua*, vol.23, pp. 287-306.

Chari, M. V. K.; Salon, S. J. (2005): Numerical Methods in Electromagnetics, Elsevier Science Ltd., Holland.

Chen, B.; Peng, X.; Chen, X.; Wang, J.; Wang, H.; Hu, N. (2012): A three-dimensional model of shape memory alloys under coupled transformation and plastic deformation. *CMC-Computers, Materials, & Continua*, vol. 30, pp. 145-176.

Honig, J. M. (1999): Thermodynamics, Academic Press, London.

Kanca, E.; Eskil, M. (2009) Comparison of new formulations for martensite start temperature of Fe-Mn-Si shape memory alloys using geneting programming and neural networks. *CMC-Computers, Materials, & Continua*, vol.10, pp. 65-95.

Karaca, H. E.; Karaman, I.; Basaran, B.; Lagoudas, D. C. (2007): On the stress-assisted magne- tic-field-induced phase transformation in Ni_2MnGa ferromagnetic shape memory alloys. *Acta Materialia*, vol. 55, pp. 4253-4269.

Kiang, J.; Tong L. (2007): Three-dimensional constitutive equations for Ni-Mn-Ga single crystals. *Journal of Magnetism and Magnetic Materials*, vol. 313 pp. 214-229

Kiang, J.; Tong L. (2009): Nonlinear magneto-mechanical finite element analysis of Ni-Mn-Ga single crystals. *Smart Materials and Structures*, Vol.19, pp.015017.

Kieer, B.; Lagoudas, D. C. (2005): Magnetic field-induced martensitic variant reorientation in magnetic shape memory alloys. *Philosophical Magazine*, vol. 85, pp. 4289- 4329.

Lagoudas, D. C.; Kiefer, B.; Haldar K. (2008): Magneto-mechanical finite element analysis of magnetic shape memory alloys with body force and body couple.

Conference on Smart Materials, Ellicott City, Maryland, USA, vol. 10, pp. 28-30.

O'Handley, R. C. (2000): Modern Magnetic Materials: Principles and Applications, Wiley, New York.

Pei, Y. M.;Fang, D. N. (2007): A model for giant magnetostrain and magnetization in the martensitic phase of NiMnGa alloys. *Smart Materials and Structures*, vol. 16, pp. 779 -783.

Straka, L.; Heczko, O. (2003): Superelastic response of Ni-Mn-Ga martensite in magnetic fields and a simple model. *IEEE Transactions on Magnetics,* vol. 39, pp. 3402-3404.

Tickle, R. (2000): Ferromagnetic Shape Memory Materials. University of Minnesota.

Ullakko, K.; Huang, J. K. (1996): Large magnetic-field induced strains in Ni_2MnGa single crystals. *Applied Physics Letters*, vol. 69, pp. 1966-1968.

Wang, J.; Steinmann, P. (2013): Finite element simulation of the magneto-mechanical response of a magnetic shape memory alloy. *Philosophical Magazine*, vol. 9, pp. 2630-2653.

Wang, X.; Li, F.; Hu, Q. (2012): An anisotropic micromechanical-based model for characterizing the magneto-mechanical behavior of NiMnGa alloys. *Smart Materials and Structures*, vol. 21, pp. 065021.

Zhu, Y. P.; Dui, G. S. (2008): Model for field-induced reorientation strain in magnetic shape memory alloy with tensile and compressive loads. *Journal of Alloys and Compounds*, vol. 459, pp. 55-60.

Zhu, Y. P.; Shi, T.; Wang, Y. (2013): Numerical evaluation of Eshelby's tensor of anisotropic ferromagnetic shape memory alloys and its influence on magnetic field-induced strain. *Computer Modeling in Engineering & Sciences*, vol.95, pp. 471-487.

Appendix

$$[\mathbf{P}_0] = \begin{bmatrix} \frac{1}{\mu_0} & 0 & 0 & 0 & 0 & 0 \\ 0 & 1 & 0 & 0 & 0 & 0 \\ 0 & 0 & \frac{1}{\mu_0} & 0 & 0 & 0 \\ 0 & 0 & 0 & 1 & 0 & 0 \\ 0 & 0 & 0 & 0 & \frac{1}{\mu_0} & 0 \\ 0 & 0 & 0 & 0 & 0 & 1 \end{bmatrix} \quad [N] = \begin{bmatrix} N_1 & N_2 & N_3 & \cdots & N_K \\ N_1 & N_2 & N_3 & \cdots & N_K \\ N_1 & N_2 & N_3 & \cdots & N_K \end{bmatrix}$$

$$[Z]_u = \begin{bmatrix} \frac{\partial N_1}{\partial x} & 0 & 0 & \frac{\partial N_2}{\partial x} & 0 & 0 & \cdots & \frac{\partial N_K}{\partial x} & 0 & 0 \\ 0 & \frac{\partial N_1}{\partial y} & 0 & 0 & \frac{\partial N_2}{\partial y} & 0 & \cdots & 0 & \frac{\partial N_K}{\partial y} & 0 \\ 0 & 0 & \frac{\partial N_1}{\partial z} & 0 & 0 & \frac{\partial N_2}{\partial z} & \cdots & 0 & 0 & \frac{\partial N_K}{\partial z} \\ 0 & \frac{\partial N_1}{\partial z} & \frac{\partial N_1}{\partial y} & 0 & \frac{\partial N_2}{\partial z} & \frac{\partial N_2}{\partial y} & \cdots & 0 & \frac{\partial N_K}{\partial z} & \frac{\partial N_K}{\partial y} \\ \frac{\partial N_1}{\partial z} & 0 & \frac{\partial N_1}{\partial x} & \frac{\partial N_2}{\partial z} & 0 & \frac{\partial N_2}{\partial x} & \cdots & \frac{\partial N_K}{\partial z} & 0 & \frac{\partial N_K}{\partial x} \\ \frac{\partial N_1}{\partial y} & \frac{\partial N_1}{\partial x} & 0 & \frac{\partial N_2}{\partial y} & \frac{\partial N_2}{\partial x} & 0 & \cdots & \frac{\partial N_K}{\partial y} & \frac{\partial N_K}{\partial x} & 0 \end{bmatrix}$$

$$[Z]_A = \begin{bmatrix} 0 & 0 & \cdots 0 & -\frac{\partial N_1}{\partial \mathrm{z}} & -\frac{\partial N_2}{\partial \mathrm{z}} & \cdots -\frac{\partial N_k}{\partial \mathrm{z}} & \frac{\partial N_1}{\partial \mathrm{y}} & \frac{\partial N_2}{\partial \mathrm{y}} & \cdots \frac{\partial N_k}{\partial \mathrm{y}} \\ 0 & 0 & \cdots 0 & 0 & 0 & \cdots 0 & 0 & 0 & \cdots 0 \\ \frac{\partial N_1}{\partial \mathrm{z}} & \frac{\partial N_2}{\partial \mathrm{z}} & \cdots \frac{\partial N_k}{\partial \mathrm{z}} & 0 & 0 & \cdots 0 & -\frac{\partial N_1}{\partial x} & -\frac{\partial N_2}{\partial x} & \cdots -\frac{\partial N_k}{\partial x} \\ 0 & 0 & \cdots 0 & 0 & 0 & \cdots 0 & 0 & 0 & \cdots 0 \\ -\frac{\partial N_1}{\partial y} & -\frac{\partial N_2}{\partial \mathrm{y}} & \cdots -\frac{\partial N_k}{\partial \mathrm{y}} & \frac{\partial N_1}{\partial x} & \frac{\partial N_2}{\partial x} & \cdots \frac{\partial N_k}{\partial x} & 0 & 0 & \cdots 0 \\ 0 & 0 & \cdots 0 & 0 & 0 & \cdots 0 & 0 & 0 & \cdots 0 \end{bmatrix}$$